Left Ventricular Shear Strain in Model and Experiment: The Role of Myofiber Orientation

Sander Ubbink[1], Peter Bovendeerd[1], Tammo Delhaas[2,3], Theo Arts[1,2], and Frans van de Vosse[1]

[1] Eindhoven University of Technology, PO Box 513, 5600 MB Eindhoven, The Netherlands
[2] Maastricht University, PO Box 616, 6200 MD Maastricht, The Netherlands
[3] University Hospital Maastricht, PO Box 5800, 6202 AZ Maastricht, The Netherlands

Abstract. Mathematical modeling of cardiac mechanics could be a useful clinical tool, both in translating measured abnormalities in cardiac deformation into the underlying pathology, and in selecting a proper treatment. We investigated to what extent a previously published model of cardiac mechanics [6] could predict deformation in the healthy left ventricle, as measured using MR tagging. The model adequately predicts circumferential strain, but fails to accurately predict shear strain. However, the time course of shear strain proves to be that sensitive to myofiber orientation, that agreement between model predictions and experiment may be expected if fiber orientation is changed by only a few degrees.

1 Introduction

Adequate pump function of the heart relies on the function of many underlying systems, such as initiation of cardiac contraction through electrical depolarisation, exchange of oxygen, nutrients and waste products through the coronary circulation, and directioning of the blood flow through the heart valves. Malfunction of each of these systems leads to deterioration of pump function.

Many cardiac pathologies (e.g. ischemia, disturbed conduction) are reflected in abnormal deformations of the cardiac wall [11, 13, 14]. Clinically, deformation patterns of the heart can be assessed with MR tissue tagging, creating opportunities in determining the underlying pathology. However, the relation between the change in deformation pattern and the underlying pathology is not straight forward. A mathematical model, capable of predicting the forward relation between pathology and deformation, could, if used in an inverse analysis, be a useful clinical tool in determining causes of the pathology and a proper treatment.

Several models describing deformation in the heart have been proposed [2, 5, 7, 8, 12]. None of these models has already been used as a diagnostic tool. Even the first step towards this application, the complete prediction of deformation in

A.F. Frangi et al. (Eds.): FIMH 2005, LNCS 3504, pp. 314–324, 2005.

the normal healthy heart, has not been made. In this study we investigate the capability of a previously published three-dimensional finite element (FE) model of cardiac mechanics [6], to predict the deformations of the myocardial wall of the healthy left ventricle.

2 Methods

2.1 Assessment of LV Wall Strain Using MR Tagging

In four healthy subjects (age 28 to 33 years) deformation patterns of the heart were assessed noninvasively using MR tagging. The experiments were performed at the University Hospital Maastricht, in a 1.5 T scanner (Gyroscan NT, Philips Medical Systems, Best, The Netherlands), with imaging parameters set as follows: echo time 10 ms, inter-tag distance 6 mm, slice thickness 8 mm, tag-width 2.5 mm, field of view 250 mm and image size 256 × 256 pixels. Images were acquired using ECG-triggering on the R wave during breath hold for a period of about 20 s. Five parallel short-axis slices of the heart were imaged, evenly distributed from apex to base (figure 1). Series of line-tagged images from the same slices were obtained, with time intervals of about 20 ms, using spatial modulation of the magnetization [1].

From the MR-images, displacement maps were determined [13]. Next, the Green-Lagrange strain tensor was determined with respect to begin ejection, and written in components with respect to a local cylindrical coordinate system.

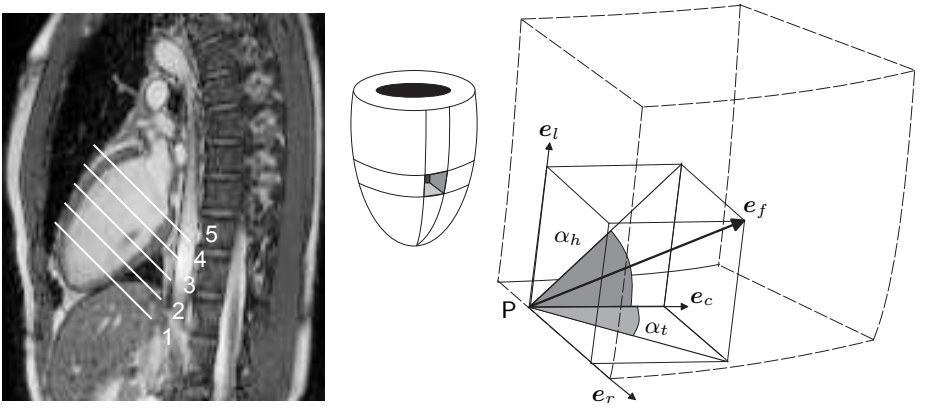

Fig. 1. Left: long-axis MR slice demonstrating the positions of the five short-axis slices, imaged in the LV of the heart, numbered from 1 (apex) to 5 (base). Right: illustration of the ellipsoidally shaped model of left ventricular mechanics showing helix (α_h) and transverse (α_t) fiber angles. The fiber angles at a point P are defined from projection of the fiber direction $\boldsymbol{e}_f$ on planes spanned by the local transmural $\boldsymbol{e}_r$, longitudinal $\boldsymbol{e}_l$ and circumferential $\boldsymbol{e}_c$ direction

Strain components were averaged in transmural direction, with weight factors distributed according to a gaussian curve with the top at the midwall position. Finally, these midwall values were averaged in circumferential direction, yielding the average circumferential (E_{cc}) and radial (E_{rr}) normal strain, and circumferential-radial shear strain (E_{cr}) for each of the five slices.

To relate timing of the MR images to phases in the cardiac cycle, for each moment in each slice the midwall radius was determined. Using the interslice distance, the volume enclosed by the ventricular midwall was estimated. Differentiation of this volume with respect to time yielded an estimation of mitral inflow and aortic outflow. Zero crossings of this signal defined moments of transition between phases in the cycle.

2.2 Computation of LV Wall Strain Using the FE Mechanics Model

The finite element (FE) model of LV mechanics has been described before [6]. In short, a thickwalled geometry is assumed with endocardial and epicardial surfaces consisting of confocal ellipsoids. The helix angle α_h and transverse angle α_t are used to describe the base-to-apex component and the transmural component of the myofiber direction, respectively (figure 1). In the model, conservation of momentum is solved:

$$\boldsymbol{\nabla} \cdot \boldsymbol{\sigma} = \mathbf{0} \tag{1}$$

with $\boldsymbol{\sigma}$ representing the Cauchy stress, composed of a passive component ($\boldsymbol{\sigma}_p$) and an active component (σ_a) along the myofiber direction $\boldsymbol{e}_f$:

$$\boldsymbol{\sigma} = \boldsymbol{\sigma}_p + \sigma_a \boldsymbol{e}_f \boldsymbol{e}_f \tag{2}$$

Passive material behaviour is modeled nonlinearly elastic, transversely isotropic and virtually incompressible. The active stress σ_a is assumed to depend on time elapsed since depolarization, sarcomere length and sarcomere shortening velocity. Depolarization is assumed to be simultaneous.

Several simulations were performed. In the simulation, indicated with ref, settings of α_h and α_t were adopted from Rijcken et al. [9, 10], who determined myofiber orientation by optimization for a homogenous distribution of fiber strain during ejection (figure 2). In view of reported sensitivity of wall mechanics to fiber orientation [2, 4], sensitivity of computed strains to settings of α_t and α_h was investigated. Sensitivity to the choice of α_t was assessed in simulations trans-2 and trans+2, where α_t was shifted by -2^o and $+2^o$, and simulations trans*0.75 and trans*1.25, where α_t was multiplied by 0.75 and 1.25. Similar variations were applied to the helix angle α_h: in simulations helix-5 and helix+5 α_h was shifted by -5^o and $+5^o$, whereas in simulations helix*0.9 and helix*1.1 α_t was multiplied by 0.9 and 1.1 (figure 2). The variations were chosen such, that the resulting distributions of the fiber angles were within the range of experimental data.

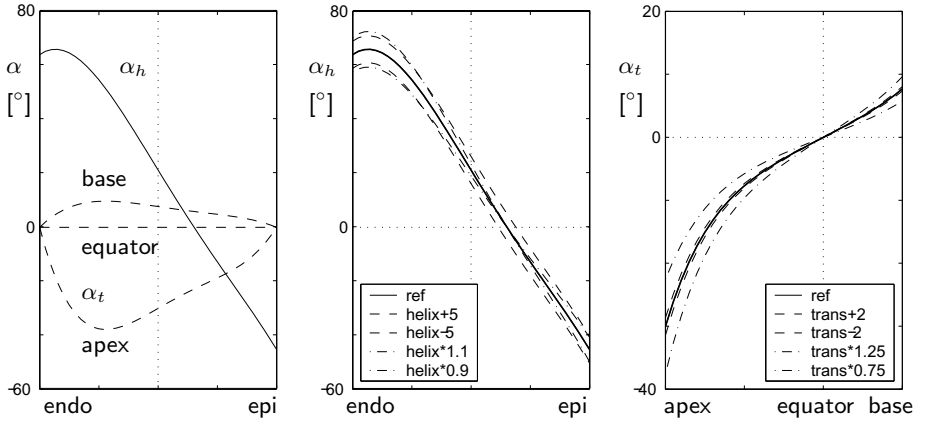

Fig. 2. Left: variation of the helix angle α_h (—) at the equator, and transverse angle α_t (- -) at base, equator and apex, from endocardial to epicardial surface, as in the reference simulation; middle: transmural variation of α_h at the equator for various simulations; right: base-to-apex variation of α_t at the midwall for various simulations

3 Results

3.1 LV Wall Strain Assessed with MR Tagging

Images were acquired over a time span of 600 ms. Since the cardiac cycle time was about 750 ms, no strains were determined for the last part of the filling phase and the initial part of the isovolumic contraction phase. Measured circumferential strain E_{cc} was similar in all four hearts. Typically, E_{cc} was similar in all five

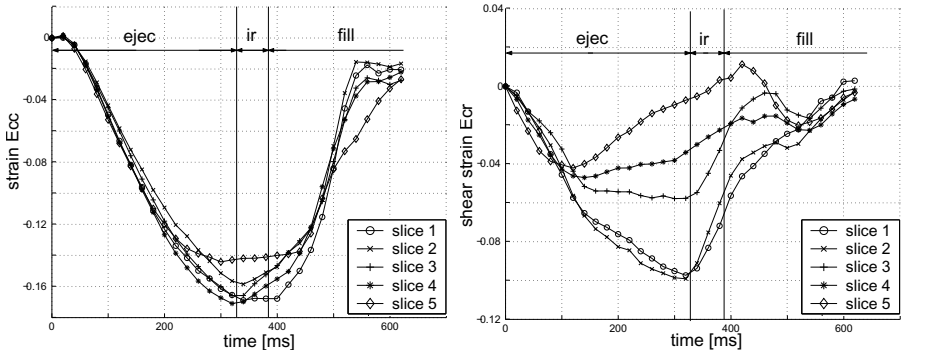

Fig. 3. Representative measured time courses of left ventricular midwall circumferential (left) and circumferential-radial shear (right) strain. Slices are numbered from apex (slice 1) to base (slice 5). Phases are indicated by ejec (ejection) ir (isovolumic relaxation) and fill (filling)

slices (figure 3). Measured shear strain E_{cr} was similar in 3 out of 4 hearts. Typically, E_{cr} decreased equally in all five slices until one third of the ejection period (figure 3). Thereafter, E_{cr} continued decreasing near the apex (slice 1), remained about constant near the equator (slice 3), and increased near the base (slice 5). Throughout the isovolumic relaxation phase, E_{cr} increased in all slices. During the first part of filling, E_{cr} converged towards the state at begin ejection in all slices.

3.2 LV Wall Strain Computed with the Reference Model

Time courses of strains E_{cc} and E_{cr} with respect to begin ejection, as computed in the ref simulation at lattitudes corresponding to slices 2 to 4 are shown in the left panel of figure 4. To facilitate comparison, the experimental data are

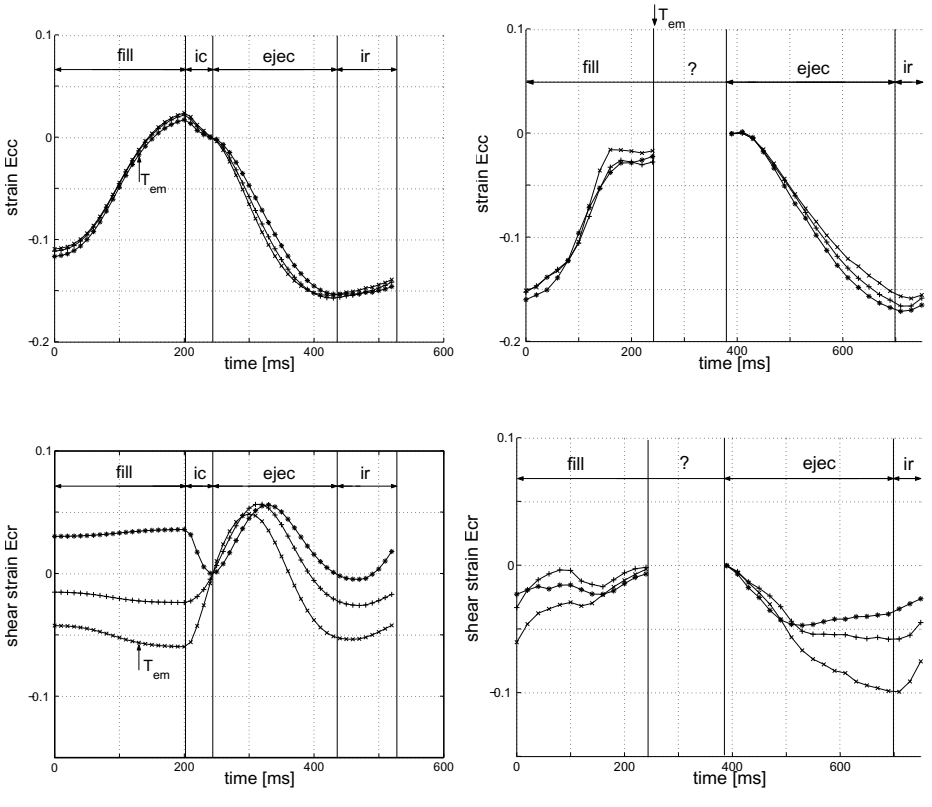

Fig. 4. Time courses of circumferential strain E_{cc} (top) and circumferential-radial strain E_{cr} (bottom) as predicted by the LV mechanics model according to the ref simulation (left) and as measured (right) for slices 2 ($\times$), 3 ($+$) and 4 ($\star$). Phases are indicated by fill (filling), ic (isovolumic contraction), ejec (ejection), and ir (isovolumic relaxation). No experimental data are available in the period indicated by ?

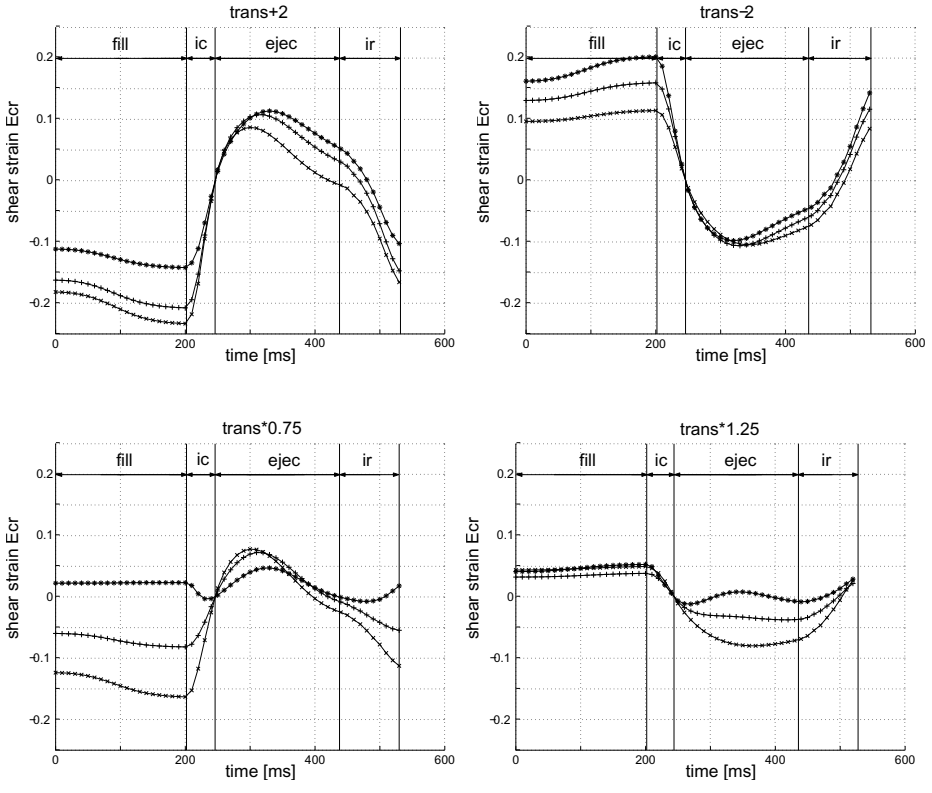

Fig. 5. Time courses of midwall E_{cr} for slices 2 ($\times$), 3 ($+$) and 4 ($\star$), as predicted by the LV mechanics model, according to simulations trans+2, trans-2, trans*0.75 and trans*1.25, representing for various settings of the transverse fiber angle. Note that range of the strain axis is twice the range of the strain axis in figure 4

redrawn in the right panel. The model predicts a virtually identical time course of E_{cc} for all three slices. E_{cc} increases during filling, decreases slightly during isovolumic contraction, decreases further during ejection, and remains nearly constant during isovolumic relaxation. The pattern is similar to the measured pattern, including the overall increase in strain from T_{em}, the moment the last MR image was acquired, to begin ejection.

In the model, E_{cr} is about constant during filling, with a small decrease for slices 2 and 3, and a small increase for slice 4 towards the end of filling. During isovolumic contraction, E_{cr} increases in slices 2 and 3 and decreases in slice 4. During the first part of ejection, E_{cr} increases similarly for the three slices. Thereafter, E_{cr} values decrease and diverge. During isovolumic relaxation, E_{cr} values increase towards the values at the beginning of filling.

Computed E_{cr} is quite different from measured E_{cr}. In particular, the model predicts a strong change of E_{cr} from T_{em} until begin of ejection, while variation

in the experiment is negligible. During the first part of ejection, changes in E_{cr} in model and experiment are opposite.

3.3 Sensitivity of LV Wall Strain to Fiber Orientation

Simulations trans+2 en trans-2 illustrate that a change in offset in α_t predominantly affects the common change in E_{cr} in all three slices during isovolumic contraction and the beginning of the ejection (figure 5; top panels). A change in the slope of the longitudinal course of α_t (simulation trans*0.75 and trans*1.25) affects the differences in E_{cr} between the slices during isovolumic contraction (figure 5; bottom panels).

A change in offset of the helix angle distribution (simulations helix+5 and helix-5) changes the range in E_{cr} during ejection (figure 6; top panels) moderately. A change in slope of the transmural course of α_h (simulations helix*0.9 and helix*1.1) has a small effect on the distribution of changes in E_{cr} during isovolumic contraction (figure 6; bottom panels).

4 Discussion

Left ventricular wall strains, as predicted by an existing model of left ventricular mechanics, were compared with strains, derived from MR tagging measurements in healthy humans. Differences between measured and computed time course of E_{cc} in the equatorial region of the LV were small, but the differences in E_{cr} appeared significant. This is not surprising, since the change of E_{cc} is closely related to the change in cavity volume, while E_{cr} is related to the internal equilibrium of forces in the LV wall. Discrepancies in E_{cr} occurred predominantly between the moment of end of measurement T_{em} and about mid ejection. In the model, E_{cr} changed strongly during isovolumic contraction, when the LV transforms from the passive diastolic to the active systolic state. Apparently, mechanical equilibrium in the anisotropic activated tissue involves large forces in the passive matrix, and consequently a large deformation. In contrast, in the experiment, E_{cr} at T_{em} was about equal to that at the beginning of ejection. During the period from T_{em} until the end of isovolumic contraction, E_{cr} was not measured. However, E_{cr} at T_{em} may be considered representative for strain at end diastole: during the last part of the filling phase no shear deformation is to be expected since the tissue is passive and hence virtually isotropic. This expectation is supported by the time derivative of measured E_{cr} near T_{em}, which is about zero. Although no strains were measured during isovolumic contraction, the data suggest that no significant deformation of the passive matrix occurs during this phase either.

The parameter variations show that the extent to which the passive matrix is involved in force transmission is very sensitive to the orientation of the muscle fibers. The influence of the helix angle α_h and the transverse α_t on shear E_{cr} is illustrated in figure 7. As a consequence of the base-to-apex component of fiber orientation, expressed by α_h, shortening of subendocardial myofibers would cause

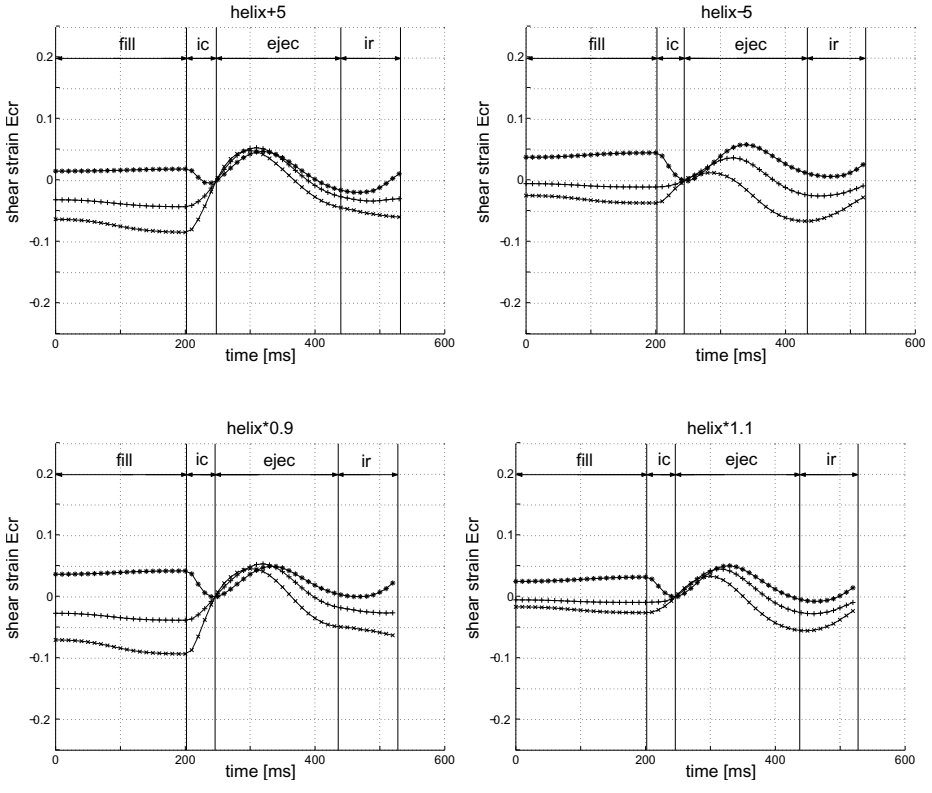

Fig. 6. Time course of the midwall E_{cr} for slices 2 ($\times$), 3 ($+$) and 4 ($\star$) as predicted by LV mechanics model according to simulations helix+5, helix-5, helix*0.9 and helix*1.1, representing various settings of the helix fiber angle

a clockwise apical rotation, when viewing the apex in apex-to-base direction. Shortening of subepicardial myofibers would cause a counterclockwise apical rotation. In the absence of an endo-to-epi component of fiber orientation, this shear load can only be counteracted by the passive myocardial tissue. Because the passive tissue has a low stiffness, mechanical equilibrium is reached at large shear strains E_{cr}. If, however, myofibers cross over between inner and outer layers of the wall, as expressed by a nonzero α_t, then these active, relatively stiff myofibers participate in the transmission of the shear load as well, and shear deformation is reduced. The role of the transverse angle has been identified before [2], but no realistic prediction of LV wall shear was obtained in that study.

Our study has its limitations. Strains are averaged in circumferential and radial direction, which reduces noise but also removes information on strain gradients in these directions. Circumferential averaging is in line with the rotational symmetry of our model of LV mechanics. Probably computed shear strains are less sensitive to geometry [4] than to timing of depolarization of the LV wall [6]

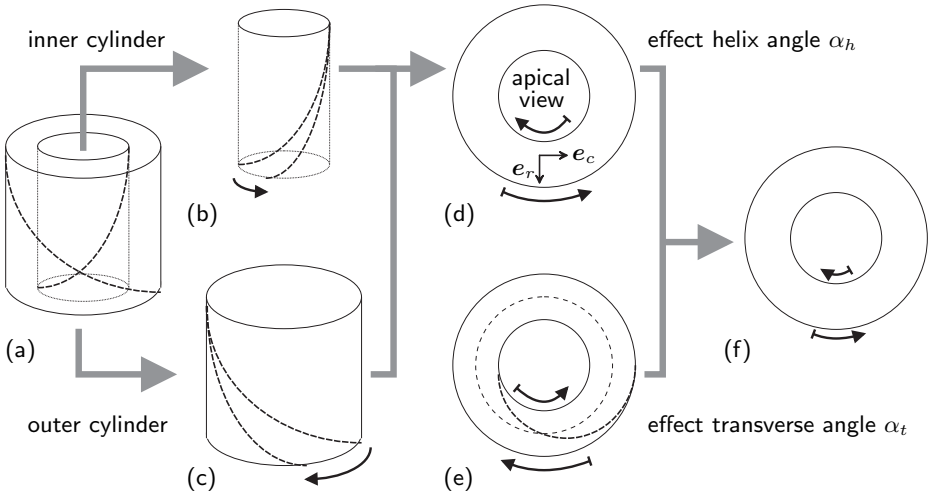

Fig. 7. Schematic illustration of the influence of helix angle α_h and transverse angle α_t on transmural shear in a cylindrical model of the LV. In absence of a transverse angle (a), shortening of the myofibers (**- - -**) would cause a clockwise apical rotation of the endocardium (b) and a counterclockwise rotation of the epicardium (c). In the commonly used apex-to-base view of short-axis images, this results in a positive circumferential-radial shear (d), i.e. the angle between line elements originally oriented in circumferential ($\boldsymbol{e}_c$) and radial ($\boldsymbol{e}_r$) direction will become less than 90°. This shear is counteracted by a negative circumferential-radial shear, as a result of the negative transverse angle in the apical part of the ventricle (e). The final shear (f) depends on the balance between the two effects

or passive shear stiffness. While the latter aspects remain to be investigated, we expect the sensitivity of shear strain to myofiber orientation to persist.

In literature, other models of the cardiac mechanics have been proposed [5, 7, 12], but none of them yielded an accurate representation of measured shear strains. Discrepancies were attributed to simplifying orthotropic passive behaviour to transversely isotropic behaviour [5], but sensitivity of the computed deformations to the choice of the passive material model was small [12]. Also, it was suggested that active cross-fiber stress development should be incorporated into the models. Indeed, introduction of active cross-fiber stress affected end-systolic shear strains significantly, but agreement with experimental values was not obtained [12].

The present study suggests that the main shortcoming in the above models lies in an unrealistic setting of myofiber orientation, in particular in neglecting the transmural component of myofiber orientation, expressed by a non-zero transverse angle. With histological sectioning techniques, fiber angles are obtained with an accuracy of ±10°. When using magnetic resonance diffusion tensor imaging, accuracy is about ±6° [3]. Our sensitivity study shows that the

reliability of experimental data is too low to be able to yield reliable predictions of LV wall strain.

5 Conclusion

It is concluded that (1) the previously published three-dimensional mathematical model of cardiac mechanics [6] adequately predicts circumferential strain, but fails to accurately predict shear strain, (2) the time course of shear strain is very sensitive to the choice of the myofiber orientation, in particular to the choice of the transverse angle, and (3) agreement between model predictions and experiment may be expected by a change of the fiber orientation by only a few degrees.

References

1. Axel L. MR imaging of motion with spatial modulation of magnetization. *Radiology*, 171:841–845, 1989.
2. Bovendeerd P.H.M., Huyghe J.M., Arts T., van Campen D.H., Reneman R.S. Influence of endocardial-epicardial crossover of muscle fibers on left ventricular wall mechanics. *J. Biomech.*, 27:941–951, 1994.
3. Geerts L., Bovendeerd P.H.M., Nicolay K., Arts T. Characterization of the normal cardiac myofiber field in goat measured with MR diffusion tensor imaging. *Am. J. Physiol.*, 283, H126–H138, 2002.
4. Geerts-Ossevoort L., Kerckhoffs R.C.P., Bovendeerd P.H.M., and Arts T. Towards patient specific models of cardiac mechanics: a sensitivity study, in *Functional Imaging and Modeling of the Heart* Ed. Magnin I.E., Montagnat J., Clarysse P., Nenonen J., Katila T., Lyon, France, 81-90, 2003.
5. Guccione J.M., Costa K.D., McCulloch A.D. Finite element stress analysis of left ventricular mechanics in the beating dog heart. *J. Biomech.*, 10:1167–1177, 1995.
6. Kerckhofs R.C.P., Bovendeerd P.H.M., Kotte J.C.S., Prinzen F.W., Smits K., Arts T. Homogeneity of cardiac contraction despite physiological asynchrony of depolarization: a model study. *Ann. Biomed. Eng.*, 31:536–547, 2003.
7. Nash M. *Mechanics and material properties of the heart using an anatomically accurate mathematical model.* PhD thesis, University of Auckland, 1998.
8. Nash M.P., and Hunter, P.J. Computational mechanics of the heart. *J. Elast.*, 61:113–141, 2000.
9. Rijcken J. *Optimization of left ventricular muscle fiber orientation.* PhD thesis, University of Maastricht 1997.
10. J. Rijcken, P.H.M. Bovendeerd, A.J.G. Schoofs, D.H. van Campen, Arts T. Optimization of cardiac fiber orientation for homogeneous fiber strain during ejection. *Ann Biomed Eng.*, 27:289–297, 1999.
11. Stuber M., Scheidegger M.B., Fischer S.E., Nagel E., Steinemann F., Hess O.M., Boesiger P. Alterations in the local myocardial motion pattern in patients suffering from pressure overload due to aortic stenosis. *Circ.*, 100:361–368, 1999.
12. Usyk T.P., Mazhari R., McCulloch A.D. Effect of laminar orthotropic myofiber architecture on regional stress and strain in the canine left ventricle. *J. Elast.*, 61:143–164, 2000.

13. van der Toorn A., Barenbrug P., Snoep G., van der Veen F.H., Delhaas T., Prinzen F.W., Maessen J., Arts T. Transmural gradients of cardiac myofiber shortening in aortic valve stenosis patients using mri tagging. *Am. J. Physiol.*, 283:1609–1615, 2002.
14. Villarreal F.J., Lew W.Y.W., Waldman L.K., Covell J.W. Transmural myocardial deformation in the ischemic canine left ventricle. *Circ. Res.*, 689:368–381, 1991.